

Full Quantum Work Statistics for Non-Homogeneous Many-Body Systems

Antonio Palamara,^{1,2,*} Francesco Plastina,^{1,2} Antonello Sindona,^{1,2} and Irene D'Amico^{3,4}

¹*Dipartimento di Fisica, Università della Calabria, Via P. Bucci, Cubo 30C, I-87036 Rende (CS), Italy*

²*INFN, Gruppo Collegato di Cosenza, Via P. Bucci, Cubo 31C, I-87036 Rende (CS), Italy*

³*School of Physics, Engineering and Technology, University of York, YO10 5DD York, United Kingdom*

⁴*York Center for Quantum Technologies, The University of York, YO10 5DD, York, United Kingdom*

(Dated: December 23, 2025)

The nonequilibrium thermodynamics of interacting quantum many-body systems is investigated within the framework of thermal time-dependent density functional theory using a generalized linear-response formulation for the full quantum work statistics. A first-principles route is established to reconstruct the relaxation function that underlies linear-response theory, thereby moving beyond phenomenological descriptions and enabling a consistent evaluation of all moments of the dissipated-work distribution in interacting systems. The predictive power of the approach is demonstrated for the Hubbard model subject to a staggered external potential, where the evolution of the relaxation dynamics across the Mott-to-band-insulator crossover reveals how distinct many-body phases shape the out-of-equilibrium thermodynamic response. These results provide a microscopic and transferable framework for quantum thermodynamics in correlated systems, bridging thermal density functional theory and nonequilibrium work statistics.

I. INTRODUCTION

Nonequilibrium thermodynamics in quantum systems has become a central theme in modern quantum statistical mechanics and quantum information science [1–7], driven by fundamental questions concerning irreversibility and fluctuations at the quantum scale, as well as by the demands of emerging quantum technologies [8, 9]. In particular, the assessment of quantum fluctuations, which persist even in the absence of thermal noise, is essential for determining the energetic cost, performance, and stability of quantum protocols [10–17]. Over the past decade, ultracold atomic gases and trapped ions have emerged as highly controllable platforms for quantum simulations of condensed-matter phenomena [18–20]. Exploiting their intrinsic cleanliness and tunability, these systems have enabled precise experimental tests of quantum thermodynamic principles, including fluctuation relations and work statistics [21–24]. These developments underscore the need for microscopic approaches to quantum thermodynamics in interacting many-body systems, where correlations and quantum coherence play a key role in shaping both equilibrium and nonequilibrium behavior [25–29].

Density functional theory (DFT) [30, 31] and its time-dependent extension (TDDFT) [32, 33] provide a unified first-principles framework for describing interacting many-particle systems at zero temperature. Originally formulated for the electronic many-body problem, these approaches have been generalized to lattice Hamiltonians and model systems [34–44]. More recently, renewed attention has been devoted to thermal density functional theory (thDFT) [45–54] and its time-dependent extension (thTDDFT) [55, 56], motivated by the need to address finite-temperature properties and nonequilibrium processes in which thermal effects are indispensable. In this setting, several works have explored density-functional formulations of quantum thermodynamics, aiming to connect

nonequilibrium energy statistics with ground-state and time-dependent density functionals [57–60]. Notably, a thermal density-functional framework for describing work distributions in sudden-quench processes was introduced [61], providing a first-principles route to express nonequilibrium thermodynamic observables directly in terms of thermal densities and Kohn-Sham potentials.

A central open question concerns the nature and energetic impact of quantum fluctuations during finite-time thermodynamic processes. While quasi-static transformations have been extensively analyzed [62–73], extending nonequilibrium formulations beyond this limit remains highly nontrivial, particularly for interacting many-body systems [74, 75]. A significant development introduced a generalized linear-response theory (GLRT) for the full quantum work statistics [76], in which all moments of the dissipated-work distribution are expressed in terms of the relaxation function [77, 78], encoding the response of the system to an external driving protocol. When microscopic information is unavailable, the relaxation function may be modeled phenomenologically, underscoring the versatility of the framework, albeit at the expense of predictive accuracy.

In this work, a further advancement of this frontier is presented by deriving the relaxation function directly from microscopic first principles, thereby providing a predictive and transferable approach to quantum thermodynamic processes in interacting many-body systems. Specifically, linear-response thermal time-dependent density functional theory (LR-thTDDFT) is employed to obtain accurate approximations of the relaxation function and, consequently, of the full work distribution. The applicability of the approach is illustrated for the Hubbard model in a staggered external potential by analyzing the first moments of the dissipated-work distribution across the Mott-to-band-insulator crossover.

In principle, thDFT and thTDDFT are formally exact; however, in practice, both equilibrium and nonequilibrium calculations rely on approximate exchange-correlation functionals [79, 80]. Here, using the thermal adiabatic local density approximation (thALDA) [55], it is shown that even a local

* corresponding author: antonio.palamara@unical.it

and temporally adiabatic kernel captures the essential role of many-body phases in shaping the nonequilibrium thermodynamics of the interacting system.

II. FULL QUANTUM WORK STATISTICS IN LINEAR RESPONSE

To set the stage, consider a generic quantum system driven by a time-dependent external potential through the Hamiltonian

$$\hat{H}(t) = \hat{H}_0 + \lambda(t) \hat{V}, \quad (1)$$

where $\lambda(t)$ varies over the interval $[0, \tau]$ and defines the driving protocol. The operator \hat{V} acts as a perturbation that is effectively switched on at $t = 0$ and switched off at $t = \tau$. Accordingly, the work parameter changes from $\lambda(0) = 0$ to $\lambda(\tau) = \delta\lambda$, with an average rate proportional to $1/\tau$. The system is initially prepared in the thermal equilibrium state of \hat{H}_0 at inverse temperature β and is subsequently driven unitarily into a nonequilibrium state by the protocol $\lambda(t)$.

We focus on the dissipated-work distribution $P(W_{\text{diss}})$, which underpins the full stochastic thermodynamics of the process, and in particular on its first moment $\langle W_{\text{diss}} \rangle$, identified within the two-point measurement framework [6, 81]. The dissipated work is strictly related to the irreversibility of the process and can be expressed exactly in terms of the quantum relative-entropy functional $S(\cdot \parallel \cdot)$ [82], as

$$\beta \langle W_{\text{diss}} \rangle = S(\hat{\rho}_\tau \parallel \hat{\rho}_\tau^{\text{th}}), \quad (2)$$

where $\hat{\rho}_\tau$ denotes the nonequilibrium state after the evolution, and $\hat{\rho}_\tau^{\text{th}}$ is the thermal state toward which the system would relax at the end of the protocol [83].

A central result of the GLRT [76] is that the full dynamical response of the system is encapsulated in the *relaxation function*,

$$\psi(t) = \beta \int_0^\tau ds \langle \hat{V}(-is) \hat{V}(t) \rangle_0 - \beta^2 \langle \hat{V} \rangle_0^2, \quad (3)$$

where $\hat{V}(t) = e^{i\hat{H}_0 t} \hat{V} e^{-i\hat{H}_0 t}$ and $\langle \cdots \rangle_0$ denotes the thermal average with respect to \hat{H}_0 . This function satisfies two key constraints: time-reversal symmetry, $\psi(t) = \psi(-t)$, and the nonnegativity of its Fourier transform, $\tilde{\psi}(\omega) \geq 0$, the latter ensuring consistency with the second law of thermodynamics [84].

Furthermore, all cumulants $\{k_w^n\}$ of the dissipated-work distribution are nonnegative and can be expressed as bilinear functionals of the driving protocol through the time derivative $\dot{\lambda}(t)$:

$$\beta^n k_w^n = \int_{-\infty}^{\infty} \frac{d\omega}{\sqrt{2\pi}} \tilde{\psi}(\omega) \gamma_n(\omega) \left| \int_0^\tau dt \dot{\lambda}(t) e^{i\omega t} \right|^2. \quad (4)$$

Here, $\tilde{\psi}(\omega)$ acts as a generalized friction kernel that encodes both the linear-response behavior and the thermodynamic irreversibility, while $\{\gamma_n\}$ are model-independent coefficients of

the form

$$\gamma_n(\omega) = \frac{1}{2} (\beta\omega)^{n-1} \begin{cases} \coth(\beta\omega/2), & \text{for even } n, \\ 1, & \text{for odd } n. \end{cases} \quad (5)$$

In particular, the irreversible entropy production follows from setting $n = 1$ in Eqs. (4) and (5), leading to the convolution integral

$$\beta \langle W_{\text{diss}} \rangle = \frac{1}{2} \int_0^\tau dt \int_0^\tau dt' \psi(t-t') \dot{\lambda}(t) \dot{\lambda}(t'). \quad (6)$$

In the present work, we decompose each moment of the dissipated-work distribution into adiabatic and nonadiabatic contributions. This separation is of fundamental importance, as it allows one to distinguish irreversibility originating from the time deformation of the energy spectrum (i.e., the adiabatic one), from that arising from genuinely dissipative nonadiabatic transitions. Specifically, we show that the dissipation kernel in Eq. (6) can be expressed as a sum of adiabatic and nonadiabatic components,

$$\psi(t) = \psi_{\text{NA}}(t) + \psi_{\text{AD}}, \quad (7)$$

where ψ_{NA} contains all dynamical contributions arising from transitions between different energy levels and therefore governs genuine dissipative behavior. The fundamental reason behind this statement lies in the fact that part of the irreversibility of a thermodynamic process arises from non-adiabatic internal friction [85, 86]. The remaining portion can be quantified by the irreversibility of a hypothetical adiabatic process. The adiabatic contribution, ψ_{AD} , is independent of the driving rate, involves no transition energies, i.e., no terms proportional to $\omega \neq 0$, and reflects solely the difference between the instantaneous spectra of $\hat{H}(t)$ and $\hat{H}(0)$.

To obtain explicitly the decomposition of eq. (7), let us consider a protocol in which the Hamiltonian evolves from $\hat{H}(0)$ to $\hat{H}(\tau)$ over an infinitely long time scale, $\tau \rightarrow \infty$, such that the conditions of the adiabatic theorem are satisfied [87]. Under these conditions, the adiabatic time-evolved density matrix takes the form

$$\hat{\rho}_A = \sum_n p_n^0 |n(\tau)\rangle \langle n(\tau)|, \quad (8)$$

where $\{|n(\tau)\rangle\}$ denote the instantaneous eigenstates of the Hamiltonian at the end of the protocol ($t = \tau$), and $p_n^0 = e^{-\beta E_n(0)}/Z_0$ are the initial ($t = 0$) equilibrium occupation probabilities for the eigenstates $|n(0)\rangle \equiv |n\rangle$, with Z_0 the partition function.

For an adiabatic process, using eq.(2), one obtains

$$\begin{aligned} \beta \langle W_{\text{diss}} \rangle_{\text{AD}} &= S(\hat{\rho}_A \parallel \hat{\rho}_\tau^{\text{th}}) \\ &= \sum_n p_n^0 \ln p_n^0 + \beta \sum_n p_n^0 E_n(\tau) + \ln Z_\tau. \end{aligned} \quad (9)$$

Assuming nondegeneracy of the instantaneous spectrum, and expanding the final energy levels perturbatively up to second order in $\delta\lambda$ yields

$$E_n(\tau) = E_n(0) + \delta\lambda V_{nn} + \delta\lambda^2 \sum_{m \neq n} \frac{|V_{nm}|^2}{E_m(0) - E_n(0)}, \quad (10)$$

where $V_{nm} = \langle n|\hat{V}|m\rangle$, and, similarly, the logarithm of the partition function can be expanded as

$$\begin{aligned} \ln Z_\tau &= \ln Z_0 - \beta\delta\lambda\langle\hat{V}\rangle_0 + \frac{\beta^2\delta\lambda^2}{2}\sum_n p_n^0|V_{nn}|^2 \quad (11) \\ &\quad - \beta^2\delta\lambda^2\sum_n p_n^0\sum_{m\neq n}\frac{|V_{nm}|^2}{E_m(0)-E_n(0)} - \frac{\beta^2\delta\lambda^2}{2}\langle\hat{V}\rangle_0^2. \end{aligned}$$

Substituting Eqs. (10) and (11) into Eq. (9) gives the adiabatic contribution to the irreversible entropy production,

$$\beta\langle W_{\text{diss}}\rangle_{\text{AD}} = \frac{\delta\lambda^2\beta^2}{2}\left(\sum_n p_n^0|V_{nn}|^2 - \langle\hat{V}\rangle_0^2\right). \quad (12)$$

Recalling Eq. (6), and noting that in the adiabatic limit the nonadiabatic part of the relaxation function must vanish identically due to the absence of transition processes, we obtain a time-independent expression for the adiabatic component,

$$\psi_{\text{AD}} = \beta^2\left(\sum_n p_n^0|V_{nn}|^2 - \langle\hat{V}\rangle_0^2\right). \quad (13)$$

Consequently the nonadiabatic contribution reads

$$\psi_{\text{NA}}(t) = \beta\int_0^\beta ds\langle\tilde{V}(-is)\tilde{V}(t)\rangle_0 - \beta^2\sum_n p_n^0|V_{nn}|^2. \quad (14)$$

Finally, taking the Fourier transform of Eq. (7) yields

$$\tilde{\psi}(\omega) = \tilde{\psi}_{\text{NA}}(\omega) + \sqrt{2\pi}\delta(\omega)\psi_{\text{AD}}, \quad (15)$$

so that, using Eq. (4), the adiabatic and nonadiabatic contributions to the moments of the dissipated-work distribution can be treated separately. Owing to the structure of the coefficients $\{\gamma_n\}$, cf. Eq. (5), the adiabatic term contributes only to the first two moments, consistent with the fact that, in the slow-quench limit, the dissipated-work distribution approaches a Gaussian form.

III. RELAXATION FUNCTION FROM LR-THTDDFT MICROSCOPIC APPROACH

Building upon the GLRT framework, we now demonstrate that LR-thTDDFT can, in principle, provide a first-principles approach to the relaxation function. To keep the discussion general [61], consider a system described by the interacting Hamiltonian

$$\hat{H}[\{\lambda_i\}] = \hat{H}_0 + \hat{V}_{\text{EXT}}[\{\lambda_i(t)\}] = \hat{H}_0 + \sum_{i=1}^{\mathcal{L}} \lambda_i(t) \hat{A}_i, \quad (16)$$

where \hat{H}_0 denotes that component of \hat{H} which is independent of the external potential; i.e., in DFT terminology, the universal Hohenberg-Kohn (HK) Hamiltonian [30, 41] and \hat{V}_{EXT} represents a time-dependent external potential governed by a set of \mathcal{L} dynamic control parameters $\lambda_i(t) = [\lambda_i^0 + \delta\lambda_i(t)]$.

Here, the dependence on the index i encodes the spatial modulation of the external field, while the local operators \hat{A}_i define the corresponding coupling channels. This general form of \hat{H} encompasses a broad range of systems, including spin chains as well as fermionic and bosonic models. The central quantity in TDDFT is the time-dependent expectation value

$$a_i(t) := \text{Tr}\{\hat{\rho}(t)\hat{A}_i\}, \quad (17)$$

where $\hat{\rho}(t)$ is the unitarily evolved density operator originating from the initial grand-canonical or canonical thermal state $\hat{\rho}_\beta^{\text{th}}[\{\lambda_i\}]$. The Runge-Gross (RG) theorem [32] establishes, under fairly general conditions and with certain subtleties for lattice systems [37, 39], a one-to-one correspondence between the set of time-dependent “densities” $\{a_i(t)\}$ and the external controllers $\{\lambda_i(t)\}$, and thus with $\hat{V}_{\text{EXT}}[\{\lambda_i(t)\}]$, for a given initial state. Furthermore, the van Leeuwen theorem [56] guarantees the existence of a non-interacting reference system evolving under an effective potential that reproduces the same density dynamics as the interacting system. This potential, referred to as the time-dependent Kohn-Sham (KS) potential, incorporates both the external driving and the Hartree-exchange-correlation (Hxc) contributions. In the lattice formulation, these contributions appear as site-resolved KS fields, which should not be confused with the thermodynamic work parameters, and are denoted by $\lambda_{i,\text{Hxc}}[\{a_i(t)\}]$. Accordingly, the KS work parameters take the form

$$\lambda_{i,\text{KS}}[\{a_i(t)\}] = \lambda_i(t) + \lambda_{i,\text{Hxc}}[\{a_i(t)\}], \quad (18)$$

where $\lambda_{i,\text{KS}}(t)$ is the discrete analogue of the continuum KS potential, now acting on the local operators \hat{A}_i . As a consequence, the interacting Hamiltonian (16) is replaced by the KS Hamiltonian

$$\hat{H}_{\text{KS}}(t) = \hat{H}_0^{\text{KS}} + \sum_{i=1}^{\mathcal{L}} \lambda_{i,\text{KS}}(t) \hat{A}_i, \quad (19)$$

where \hat{H}_0^{KS} plays the role of the one-body kinetic operator in the continuous TDDFT formulation and generates the non-interacting reference dynamics.

For sufficiently weak time-dependent perturbations, the system enters the linear-response regime, and the changes in the densities can be obtained through the density-density (i.e., the $\hat{A}_j\hat{A}_i$) response function, which is defined in the time domain as

$$\chi_{ij}^\beta(t) = -i\theta(t)\langle[\hat{A}_i(t), \hat{A}_j(0)]\rangle_0, \quad (20)$$

where $\theta(t)$ denotes the Heaviside step function. Its frequency-domain form reads

$$\chi_{ij}^\beta(\omega) = \sum_{n,m} p_n \left[\frac{\langle n|\hat{A}_i|m\rangle\langle m|\hat{A}_j|n\rangle}{\omega - \omega_{mn} + i0^+} - \frac{\langle n|\hat{A}_i|m\rangle\langle m|\hat{A}_j|n\rangle}{\omega + \omega_{mn} + i0^+} \right], \quad (21)$$

which generalizes the Lehmann representation [88] to finite temperatures. Here, p_n is the thermal occupation probability of the n th eigenstate of the Hamiltonian (16) and $\omega_{mn} = E_m - E_n$ are the corresponding energy differences. The

single-particle density (\hat{A}_i)-density (\hat{A}_j) response function for the non-interacting KS system, $\chi_{ij\text{KS}}^\beta(\omega)$, can be defined in an analogous manner. The strength of the KS framework lies in the fact that, in the linear-response regime, the interacting response function can be obtained from the KS one through the Gross-Kohn (GK) formalism [55, 89], leading to the frequency-domain response equation

$$\chi^\beta(\omega) = \chi_{\text{KS}}^\beta(\omega) + \chi_{\text{KS}}^\beta(\omega) * \mathbf{f}_{\text{Hxc}}^\beta(\omega) * \chi^\beta(\omega), \quad (22)$$

where spatial indices have been omitted for clarity, bold symbols denote matrices in the site indices, and $*$ indicates matrix convolution. Equation (22) represents a formally exact Dyson-like relation that connects the interacting response function to its KS counterpart via the finite-temperature Hxc kernel $\mathbf{f}_{\text{Hxc}}^\beta(\omega)$ [33], which is defined as

$$\mathbf{f}_{\text{Hxc}}^\beta(\omega) = [\chi_\beta(\omega)]^{-1} - [\chi_{\text{KS}}^\beta(\omega)]^{-1}. \quad (23)$$

Following the Kubo-formula approach, the response function, in particular its non-adiabatic component, can be directly related to the relaxation function through its time derivative [77, 78, 90]:

$$\begin{aligned} \frac{d\psi(t)}{dt} &= \frac{d\psi_{\text{NA}}(t)}{dt} = -i\beta \langle [\tilde{V}(t), \tilde{V}(0)] \rangle_0 \\ &= -i\beta \sum_{ij} \langle [\hat{A}_i(t), \hat{A}_j(0)] \rangle_0. \end{aligned} \quad (24)$$

On the other hand, the same *density-density* response function has been given in Eq. (20). Comparing the Fourier transforms of Eqs. (24) and (21) yields a direct correspondence between $\tilde{\psi}_{\text{NA}}(\omega)$ and $\chi_\beta(\omega)$,

$$\tilde{\psi}_{\text{NA}}(\omega) = 2\beta \sum_{ij} \frac{\text{Im} \chi_{ij}^\beta(\omega)}{\omega}. \quad (25)$$

Thus, the nonadiabatic component of the relaxation function is determined by the imaginary part of $\chi_{ij}^\beta(\omega)$. This could have been expected, as $\text{Im} \chi_{ij}^\beta(\omega)$ directly reflects the transition probabilities mediated by the operators \hat{A}_i . Upon comparing Eqs. (15) and (25), the total relaxation function in the frequency domain for a nonhomogeneous many-body system can be expressed as

$$\tilde{\psi}(\omega) = 2\beta \sum_{ij} \frac{\text{Im} \chi_{ij}^\beta(\omega)}{\omega} + \sqrt{2\pi} \delta(\omega) \psi_{\text{AD}}, \quad (26)$$

where the $\delta(\omega)$ contribution arises from the time-independent adiabatic component ψ_{AD} in Eq. (13), which is independent of both time and quench rate, carries no transition energies and therefore contributes only at zero frequency. By virtue of the HK and KS theorems, the second term in Eq. (13), being a sum of products of thermal densities, is, in principle, exact when evaluated within the KS system, whereas the first term must be approximated. One possible strategy is to estimate the

leading nontrivial contribution using many-body perturbation theory, taking the KS system as the reference. Alternatively, a useful formal expression for ψ_{AD} can be obtained by exploiting the result for the irreversible entropy production in a sudden-quench protocol [61]:

$$\beta k_w^1 = -\frac{\beta^2}{2} \sum_{ij} \delta\lambda_i \delta\lambda_j \frac{\partial a_i^{\beta,0}}{\partial \lambda_j^0}, \quad (27)$$

where $a_i^{\beta,0} = \text{Tr} \{ \hat{\rho}_\beta^{\text{th}}[\{\lambda_i^0\}] \hat{A}_i \}$ is the equilibrium thermal density.

For simplicity, and unless otherwise stated, we consider a protocol in which all control channels in Eq. (16) share the same time dependence, i.e., $\lambda_i(t) = [\lambda_0 + \delta\lambda(t)] g_i$, while g_i is employed to encode the spatial pattern. Eq. (27) coincides with the irreversible entropy production obtained from Eq. (4) in the $\tau \rightarrow 0$ limit for $n = 1$. Solving the resulting equality for ψ_{AD} yields

$$\begin{aligned} \psi_{\text{AD}} &= -\frac{\beta^2 \delta\lambda^2}{b(0)} \sum_{ij} g_i g_j \frac{\partial a_i^{\beta,0}}{\partial \lambda_j} \\ &\quad - 2\beta \sum_{ij} g_i g_j \int \frac{d\omega}{\sqrt{2\pi}} \frac{\text{Im} \chi_{ij}^\beta(\omega)}{\omega} \frac{b(\omega)}{b(0)}, \end{aligned} \quad (28)$$

where

$$b(\omega) = \lim_{\tau \rightarrow 0} \left| \int_0^\tau dt \dot{\lambda}(t) e^{i\omega t} \right|^2, \quad (29)$$

represents the spectral weight of the driving protocol, quantifying how the sudden temporal profile of the control parameter distributes energy across frequencies and couples to the intrinsic excitation modes of the system. Note that $b(\omega)$ depends solely on the driving protocol and is independent of the system Hamiltonian.

To summarize, LR-thTDDFT provides the relaxation function by: (i) computing the KS response function, (ii) dressing it via the Hxc kernel to obtain the interacting response, (iii) extracting the imaginary part of $\chi_{ij}^\beta(\omega)$ through Eq. (25), and (iv) combining the nonadiabatic component with the static adiabatic term to yield the full $\tilde{\psi}(\omega)$.

It is worth stressing that everything derived up to this point is formally exact, at least within the linear-response regime. In practice, however, approximations are required at two distinct levels. The first concerns the Hxc potential, controlled by $\lambda_{i,\text{KS}}[\{a_i(0)\}]$, which enters the self-consistent equilibrium calculation of the KS Hamiltonian $\hat{H}_{\text{KS}}[\{\lambda_{i,\text{KS}}(0)\}]$ in Eq. (19) and the corresponding response function $\chi_{\text{KS}}^\beta(\omega)$. The second pertains to the quality of the approximation adopted for the dynamical Hxc kernel, defined in Eq. (23). The most widely used approximation is the thermal adiabatic local-density approximation (thALDA) [55], where the kernel is instantaneous in time; i.e., $f_{\text{Hxc}}^\beta(\omega) \approx f_{\text{Hxc}}^\beta$, which will be employed in the rest of this work.

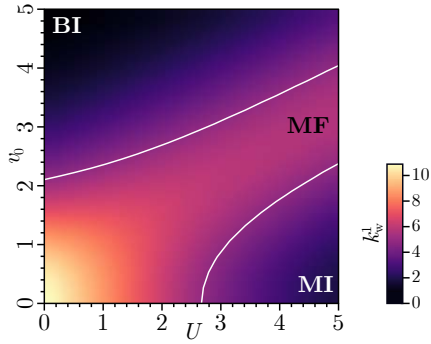


FIG. 1. Phase diagram of the Hubbard model with a staggered field, obtained from the dissipated work, $\beta \frac{\langle W_{\text{diss}} \rangle}{(\delta v)^2}$, following a sudden quench of the work parameters. Results are shown for inverse temperature $\beta J = 1$ and quench amplitude $\delta \lambda = 0.01J$ for a half-filled chain of length $\mathcal{L} = 50$. The solid line, corresponding to the 45% contour of the maximum value, serves as a visual guide to distinguish the MI, metallic (M), and BI phases.

IV. OUT-OF-EQUILIBRIUM QUANTUM THERMODYNAMICS OF THE HUBBARD MODEL

The Hubbard model [91] provides an ideal testbed for the LR-thTDDFT framework developed in the previous section. It can be experimentally realized in ultracold atomic gases using a superlattice potential [92] and captures a wide variety of correlated-electron phenomena.

To keep the discussion focused, we consider the half-filled case with total spin projection along the z axis equal to zero, subject to a time-dependent external potential. The Hamiltonian for a finite chain of length \mathcal{L} has the form

$$\hat{H}(t) = \hat{T} + \hat{W} + \hat{V}_{\text{ext}}(t), \quad (30)$$

where

$$\hat{T} = -J \sum_{i=1}^{\mathcal{L}} \sum_{\sigma=\uparrow, \downarrow} \left(\hat{c}_{i,\sigma}^\dagger \hat{c}_{i+1,\sigma} + \text{h.c.} \right) \quad (31)$$

is the kinetic hopping term,

$$\hat{W} = U \sum_{i=1}^{\mathcal{L}} \hat{n}_{i,\uparrow} \hat{n}_{i,\downarrow} \quad (32)$$

is the on-site Hubbard interaction, and

$$\hat{V}_{\text{ext}}(t) = \sum_{i=1}^{\mathcal{L}} v_i(t) \hat{n}_i, \quad v_i(t) = v(t) (-1)^i, \quad (33)$$

is a staggered, time-dependent external potential characterized by the work parameter $v(t) = v_0 + \frac{\delta v t}{\tau}$, which drives the system out of equilibrium over the interval $t \in [0, \tau]$, with $\delta v_i = \delta v (-1)^i$ and $\delta v \ll v_0$. In Eqs. (30)-(33), $\hat{c}_{i,\sigma}^\dagger$, $\hat{c}_{i,\sigma}$, and $\hat{n}_{i,\sigma}$ denote the creation, annihilation, and number operators for a fermion at site i with spin $\sigma = \uparrow, \downarrow$, respectively, while

$\hat{n}_i = \hat{n}_{i,\uparrow} + \hat{n}_{i,\downarrow}$ is the total number operator at site i . The model Hamiltonian (30) exhibits precursors of both the Mott metal-insulator transition, which favors single occupation of sites and leads to the Mott-insulating (MI) phase, and the ionic insulator transition, which promotes double occupancy under the influence of the external potential, giving rise to the band-insulating (BI) phase [93–95]. The delicate balance between the electron-electron interaction (32) and the external staggered potential (33) results in a competition between the tendencies driving the MI and BI phases, producing a metallic phase in the narrow region where $U \sim 2v_0$.

In the following, we show that LR-thTDDFT provides direct access to this interplay, enabling the exploration of the system's nonequilibrium quantum thermodynamics from the sudden-quench regime to the adiabatic limit, in the vicinity of a phase-transition precursor. We specialize to the spin-independent density-density response function $\chi_{ij}(t) = -i \theta(t) \langle [\hat{n}_i(t), \hat{n}_j] \rangle_0$, as given in Eq. (20), and adopt the thALDA form

$$f_{\text{Hxc}}^{\beta,ij}[n_i^\beta] = \frac{\partial v_{\text{Hxc}}^\beta[n_i^\beta]}{\partial n_j^\beta} \delta_{ij}, \quad (34)$$

for the Hxc kernel, derived from the Hxc potential

$$v_{\text{Hxc}}^\beta[n_i^\beta] = U + \frac{1}{\beta} \ln \Gamma_U^\beta[n_i^\beta], \quad (35)$$

recently introduced to describe the quantum thermodynamics of the Hubbard model in the sudden-quench regime [61], where

$$\Gamma_U^\beta[n_i^\beta] = \frac{(n_i^\beta - 1) + \sqrt{(n_i^\beta - 1)^2 + e^{-\beta U} [1 - (n_i^\beta - 1)^2]}}{n_i^\beta}. \quad (36)$$

Under this approximation, the exchange-correlation kernel becomes frequency independent. As a consequence, the theory neglects memory effects and, crucially, cannot describe excitonic features beyond single particle hole-excitation that may arise in correlated many-body systems. In other words, within this approximation, the number of poles in the interacting density-density response function coincides with that of the noninteracting Kohn-Sham system. Though Eq. (34) neglects nonlocal correlations in both space and time, it still yields highly accurate results, in excellent agreement with exact diagonalization of the two-site Hubbard model, as shown in Appendix A.

The starting point for obtaining the relaxation function from the density-density response function within LR-thTDDFT is the self-consistent diagonalization of the KS Hamiltonian,

$$\hat{H}_{\text{KS}} = \hat{T} + \sum_i v_i^{\text{KS}}[n_i^\beta] \hat{n}_i, \quad (37)$$

which provides the equilibrium thermal occupations of the initial Hubbard Hamiltonian $\hat{H}(0)$ in Eq. (30). The KS system is constructed in the same ensemble as the interacting system. The thermal site occupations are given by

$$n_i^\beta = -\frac{2}{\beta} \frac{\partial \ln Z_N^{\text{KS}}}{\partial v_i^{\text{KS}}}, \quad (38)$$

where $v_i^{\text{KS}}[n_i^\beta]$ denotes the KS potential and Z_N^{KS} is the grand-canonical partition function of the KS system with N_\uparrow spin-up and N_\downarrow spin-down fermions, such that $N = N_\uparrow + N_\downarrow$. Consistent with the thALDA form in Eq. (34), we adopt a thermal local-density approximation (thLDA) constructed from the Hxc functional of Eq. (35),

$$v_i^{\text{KS}}[n_i^\beta] \simeq v_i + v_{\text{Hxc}}^\beta[n_i^\beta], \quad (39)$$

On the simulation side, we considered chains of length $\mathcal{L} = 50$ with an average particle number $N = 50$. As a first step, we analyzed the irreversibility generated by a sudden quench of the external potential, $v_i(0) \rightarrow v_i(0) + \delta v_i$, starting from a grand-canonical Gibbs state. Figure 1 shows the behavior of the first moment of the dissipated work in the (U, v_0) plane,

$$\beta \frac{\langle W_{\text{diss}} \rangle}{(\delta v)^2} = -\frac{\beta^2}{2} \sum_{ij} (-1)^{i+j} \frac{\partial n_i^\beta}{\partial v_j}. \quad (40)$$

The irreversible entropy production exhibits a pronounced peak that correctly traces the crossover between MI and BI and serves as a thermodynamic signature of the metallic region. This peak originates from the enhanced susceptibility of the thermal densities to small changes in the work parameter v_0 in the vicinity of the competing MI and BI phases ($U \sim 2v_0$).

The overall topology of the diagram is consistent with known phase diagrams of the ionic Hubbard model, as obtained from density-matrix renormalization-group and mean-field approaches [93–95].

Next, we extend the analysis beyond the sudden-quench regime by incorporating finite-time evolution effects within linear response, approximating the relaxation function in Eq. (26) using the thALDA scheme.

Figures 2(a)–2(c) show the first three cumulants of the dissipated-work distribution for $U = 1$ as functions of the quench duration τ and for different initial amplitudes of the external potential v_0 . All three cumulants display a clear crossover between the nonadiabatic and adiabatic regimes. In particular, the third cumulant vanishes at fixed U for $\tau \gg \tau^*(v_0)$, consistent with the expectation that, in the adiabatic limit of linear-response theory, the dissipated-work distribution (generally non-Gaussian in character) approaches a Gaussian form, leaving only the first two cumulants nonzero.

The first and second cumulants, however, retain clear signatures of the transition from the metallic phase to the band-insulator phase, which persist even in the adiabatic regime. This behavior originates from the adiabatic contribution $\beta k_{\text{W AD}}^1$ to the irreversible work and to the second cumulant $\beta^2 k_{\text{W AD}}^2$ of its distribution, expressed as

$$\begin{aligned} \beta^m k_{\text{W AD}}^m &= -m\beta^m \sum_{ij} \delta v_i \delta v_j \frac{\partial n_i^{\beta,0}}{\partial v_j} \\ &\quad - 2m\beta^m \sum_{ij} g_i g_j \int \frac{d\omega}{\sqrt{2\pi}} \frac{\text{Im} \chi_{ij}(\omega)}{\omega} b(\omega), \end{aligned} \quad (41)$$

for $m = 1, 2$. At the boundary between the metallic region and the BI region, this term provides a substantial contribution to the total thermodynamic irreversibility. From the behavior of all three cumulants, it can also be inferred that, in the band-insulating regime ($v_0 \gg U$), the system attains adiabaticity at faster quench rates than in either the Mott or metallic phases.

As a final remark, distributions satisfying the Evans-Searles fluctuation theorem [96] are known to be constrained by the thermodynamic uncertainty relation (TUR), which, in the linear-response regime, imposes a lower bound on the Fano factor,

$$F_W = \frac{\text{Var}(W)}{\langle W_{\text{diss}} \rangle} \geq \frac{2}{\beta}. \quad (42)$$

In contrast to the classical case, and in agreement with previous analyses [76], the TUR cannot be saturated in the presence of quantum fluctuations. To examine this behavior, we computed the Fano factor for the many-body system under study. Figure 2(d) shows its dependence on the quench duration for different initial amplitudes of the staggered potential. In the adiabatic limit (for quench times longer than the system relaxation time and at fixed temperature), F_W is indeed bounded from below by $2/\beta$, as expected. In all other regimes, however, and consistently with the generalized linear-response theory for the full quantum work statistics, this bound remains unsaturated due to quantum fluctuations.

V. CONCLUSIONS

The LR-thTDDFT strategy presented here establishes a fully microscopic and predictive framework for computing the cumulants of the dissipated-work distribution in interacting many-body systems driven by spatially inhomogeneous, time-dependent external potentials. By expressing the relaxation function directly in terms of density-density response functions, this approach provides first-principles access to the full quantum work statistics within the linear-response regime, thereby superseding phenomenological modeling strategies. A defining feature of the framework is the representation of the relaxation function through an exchange-correlation kernel, which enables the systematic incorporation of both many-body interactions and the spatial structure of the driving protocol. This formulation yields a direct and transparent connection between nonequilibrium thermodynamic irreversibility and the microscopic response properties of correlated quantum systems.

The generality and effectiveness of LR-thTDDFT are demonstrated for the one-dimensional Hubbard model under a staggered external field, where the moments of the dissipated-work distribution are evaluated from the sudden-quench regime to the adiabatic limit. Within the thALDA, distinct thermodynamic signatures of the Mott-insulating, metallic, and band-insulating phases are accurately captured in the behavior of the lowest-order cumulants. Beyond the present level of approximation, the framework naturally admits systematic improvements through the inclusion of an explicit frequency dependence in the Hartree-exchange-correlation ker-

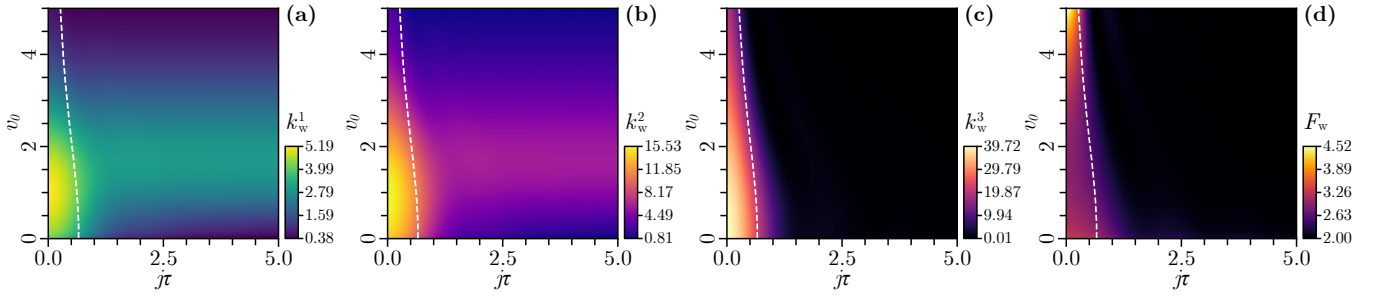


FIG. 2. (a)-(c) First three cumulants of the dissipated-work distribution for the Hubbard Hamiltonian (30) and (d) the corresponding Fano factor, plotted as functions of the quench duration τ and the staggered potential amplitude v_0 . Results are shown for inverse temperature $\beta J = 1$, quench amplitude $\delta\lambda = 0.01J$, $U = 1J$ and a half-filled chain of length $L = 50$. The dashed line $\tau^*(v_0)$ indicates the crossover between the nonadiabatic and adiabatic regimes, identified as the maximum of the absolute derivative of k_w^3 with respect to the quench time.

nel. Such extensions are expected to enable the description of many-body excitations and dynamical correlations beyond local and static limits, further enhancing the quantitative accuracy of the approach.

More generally, LR-thTDDFT provides a state-of-the-art platform for the investigation of nonequilibrium thermodynamic processes in complex quantum systems. Its scalability and microscopic grounding make it directly applicable to ultracold atomic gases and condensed-matter realizations, including low-dimensional and layered structures, where electronic correlations, spatial inhomogeneity, and geometry play a de-

cisive role in shaping the thermodynamic response.

ACKNOWLEDGEMENTS

We acknowledge N. Lo Gullo for valuable discussions during the development of this work. This research was partially supported by the Centro Nazionale di Ricerca in High-Performance Computing, Big Data and Quantum Computing, PNRR 4 2 1.4, CI CN00000013, CUP H23C22000360005, and by the PNRR MUR project PE0000023-NQSTI through the secondary projects “QuCADD” and “ThAnQ”. A.P. acknowledges support from the Erasmus+ programme.

[1] P. Talkner and P. Hänggi, Aspects of quantum work, *Phys. Rev. E* **93**, 022131 (2016).

[2] M. Campisi, P. Hänggi, and P. Talkner, Colloquium: Quantum fluctuation relations: Foundations and applications, *Rev. Mod. Phys.* **83**, 771 (2011).

[3] J. P. Pekola, Towards quantum thermodynamics in electronic circuits, *Nat. Phys.* **11**, 118 (2015).

[4] S. Vinjanampathy and J. Anders, Quantum thermodynamics, *Contemp. Phys.* **57**, 545 (2016).

[5] P. Strasberg, G. Schaller, T. Brandes, and M. Esposito, Quantum and information thermodynamics: A unifying framework based on repeated interactions, *Phys. Rev. X* **7**, 021003 (2017).

[6] M. Esposito, U. Harbola, and S. Mukamel, Nonequilibrium fluctuations, fluctuation theorems, and counting statistics in quantum systems, *Rev. Mod. Phys.* **81**, 1665 (2009).

[7] S. Campbell, I. d’Amico, M. A. Ciampini, J. Anders, N. Ares, S. Artini, A. Auffèves, L. B. Oftelie, L. Bettman, M. V. Bonançá, *et al.*, Roadmap on quantum thermodynamics, *Quantum Science and Technology* **10.1088/2058-9565/ae1e27**.

[8] N. M. Myers, O. Abah, and S. Deffner, Quantum thermodynamic devices: From theoretical proposals to experimental reality, *AVS Quantum Sci.* **4**, 027101 (2022).

[9] S. Campaioli, S. Gherardini, J. Q. Quach, M. Polini, and G. M. Andolina, Colloquium: Quantum batteries, *Rev. Mod. Phys.* **96**, 031001 (2024).

[10] F. Cleri, Quantum computers, quantum computing, and quantum thermodynamics, *Front. Quantum Sci. Technol.* **3**, 142257 (2024).

[11] J. Preskill, Quantum computing in the NISQ era and beyond, *Quantum* **2**, 79 (2018).

[12] A. Auffèves, Quantum technologies need a quantum energy initiative, *PRX Quantum* **3**, 020101 (2022).

[13] D. Jaschke and S. Montangero, Is quantum computing green? an estimate for an energy-efficiency quantum advantage, *Quantum Sci. Technol.* **8**, 025001 (2023).

[14] F. Perciavalle, N. L. Gullo, and F. Plastina, Quantum coherence and anomalous work extraction in qubit gate dynamics, arXiv:2509.09320 (2025).

[15] M. S. Blok and G. T. Landi, Quantum thermodynamics for quantum computing, *Nat. Phys.* **21**, 187 (2025).

[16] E. J. Fox, T. M. de Mendonça, F. Schmidt-Kaler, and I. D’Amico, Fractional control gate protocols for quantum engines, arXiv preprint arXiv:2509.23997 (2025).

[17] E. J. Fox, M. Herrera, F. Schmidt-Kaler, and I. D’Amico, Harnessing nth root gates for energy storage, *Entropy* **26**, 952 (2024).

[18] I. Bloch, J. Dalibard, and S. Nascimbène, Quantum simulations with ultracold quantum gases, *Nat. Phys.* **8**, 267 (2012).

[19] M. Lewenstein, A. Sanpera, V. Ahufinger, B. Damski, A. Sen, and U. Sen, Ultracold atomic gases in optical lattices: mimicking condensed matter physics and beyond, *Adv. Phys.* **56**, 243 (2007).

[20] I. Bloch, J. Dalibard, and W. Zwerger, Many-body physics with ultracold gases, *Rev. Mod. Phys.* **80**, 885 (2008).

[21] J. Koch, K. Menon, E. Cuestas, *et al.*, A quantum engine in the BEC–BCS crossover, *Nature* **621**, 723 (2023).

[22] S. Aimet, M. Tajik, G. Tournaire, *et al.*, Experimentally probing Landauer’s principle in the quantum many-body regime, *Nat. Phys.* **21**, 723 (2025).

[23] O. Onishchenko, G. Guarneri, P. Rosillo-Rodes, *et al.*, Probing coherent quantum thermodynamics using a trapped ion, *Nat. Commun.* **15**, 6974 (2024).

[24] C.-K. Hu, A. C. Santos, J.-M. Cui, *et al.*, Quantum thermodynamics in adiabatic open systems and its trapped-ion experimental realization, *npj Quantum Inf.* **6**, 73 (2020).

[25] K. T. Geier and P. Hauke, From non-Hermitian linear response to dynamical correlations and fluctuation-dissipation relations in quantum many-body systems, *PRX Quantum* **3**, 030308 (2022).

[26] D. Hahn, M. Dupont, M. Schmitt, D. J. Luitz, and M. Bukov, Quantum many-body Jarzynski equality and dissipative noise on a digital quantum computer, *Phys. Rev. X* **13**, 041023 (2023).

[27] J.-W. Zhang, B. Wang, W.-F. Yuan, *et al.*, Energy-conversion device using a quantum engine with the work medium of two-atom entanglement, *Phys. Rev. Lett.* **132**, 180401 (2024).

[28] É. Jussieu, L. Bresque, A. Auffèves, K. W. Murch, and A. N. Jordan, Many-body quantum vacuum fluctuation engines, *Phys. Rev. Res.* **5**, 033122 (2023).

[29] M. Jaramillo, M. Beau, and A. del Campo, Quantum supremacy of many-particle thermal machines, *New J. Phys.* **18**, 075019 (2016).

[30] P. Hohenberg and W. Kohn, Inhomogeneous electron gas, *Phys. Rev.* **136**, B864 (1964).

[31] W. Kohn and L. J. Sham, Self-consistent equations including exchange and correlation effects, *Phys. Rev.* **140**, A1133 (1965).

[32] E. Runge and E. K. U. Gross, Density-functional theory for time-dependent systems, *Phys. Rev. Lett.* **52**, 997 (1984).

[33] C. A. Ullrich, *Time-Dependent Density-Functional Theory* (Oxford University Press, Oxford, 2012).

[34] K. Schönhammer, O. Gunnarsson, and R. M. Noack, Density-functional theory on a lattice: Comparison with exact numerical results for a model with strongly correlated electrons, *Phys. Rev. B* **52**, 2504 (1995).

[35] L.-A. Wu, M. S. Sarandy, D. A. Lidar, and L. J. Sham, Linking entanglement and quantum phase transitions via density-functional theory, *Phys. Rev. A* **74**, 052335 (2006).

[36] C. Verdozzi, Time-dependent density-functional theory and strongly correlated systems: Insight from numerical studies, *Phys. Rev. Lett.* **101**, 166401 (2008).

[37] Y. Li and C. A. Ullrich, Time-dependent v-representability on lattice systems, *J. Chem. Phys.* **129**, 044105 (2008).

[38] I. V. Tokatly, Time-dependent current density functional theory on a lattice, *Phys. Rev. B* **83**, 035127 (2011).

[39] M. Farzanehpour and I. V. Tokatly, Time-dependent density functional theory on a lattice, *Phys. Rev. B* **86**, 125130 (2012).

[40] J. Coe, I. D’Amico, and V. V. Franca, Uniqueness of density-to-potential mapping for fermionic lattice systems, *Europhys. Lett.* **110**, 63001 (2015).

[41] V. V. Franca, J. P. Coe, and I. D’Amico, Testing density-functional approximations on a lattice and the applicability of the related Hohenberg–Kohn-like theorem, *Sci. Rep.* **8**, 664 (2018).

[42] M. Penz and R. van Leeuwen, Density-functional theory on graphs, *J. Chem. Phys.* **155**, 244111 (2021).

[43] L. Xu, J. Mao, X. Gao, and Z. Liu, Extensibility of Hohenberg–Kohn theorem to general quantum systems, *Adv. Quantum Technol.* **5**, 2200041 (2022).

[44] K. Capelle and V. L. Campo, Density functionals and model hamiltonians: Pillars of many-particle physics, *Physics Reports* **528**, 91 (2013), density functionals and model Hamiltonians: Pillars of many-particle physics.

[45] N. D. Mermin, Thermal properties of the inhomogeneous electron gas, *Phys. Rev.* **137**, A1441 (1965).

[46] K. Burke, J. C. Smith, P. E. Grabowski, and A. Pribam-Jones, Exact conditions on the temperature dependence of density functionals, *Physical Review B* **93**, 195132 (2016).

[47] A. Pribam-Jones, P. E. Grabowski, and K. Burke, Thermal density functional theory: Time-dependent linear response and approximate functionals from the fluctuation-dissipation theorem, *Physical Review Letters* **116**, 233001 (2016).

[48] J. C. Smith, A. Pribam-Jones, and K. Burke, Exact thermal density functional theory for a model system: Correlation components and accuracy of the zero-temperature exchange-correlation approximation, *Physical Review B* **93**, 245131 (2016).

[49] Z.-h. Yang, J. R. Trail, A. Pribam-Jones, K. Burke, R. J. Needs, and C. A. Ullrich, Exact and approximate kohn-sham potentials in ensemble density-functional theory, *Physical Review A* **90**, 042501 (2014).

[50] S. Pittalis, C. R. Proetto, A. Floris, A. Sanna, C. Bersier, K. Burke, and E. K. U. Gross, Exact conditions in finite temperature density functional theory, *Physical Review Letters* **107**, 163001 (2011).

[51] P. Hollebon and T. Sjostrom, Hybrid kohn-sham+thomas-fermi scheme for high-temperature density functional theory, *Physical Review B* **105**, 235114 (2022).

[52] S. Kurth and G. Stefanucci, Nonequilibrium anderson model made simple with density functional theory, *Physical Review B* **94**, 241103 (2016).

[53] V. V. Karasiev, L. Calderín, and S. B. Trickey, Importance of finite-temperature exchange correlation for warm dense matter calculations, *Physical Review E* **93**, 063207 (2016).

[54] F. Graziani, M. P. Desjarlais, R. Redmer, and S. B. Trickey, *Frontiers and Challenges in Warm Dense Matter* (Springer, 2014).

[55] A. Pribam-Jones, P. E. Grabowski, and K. Burke, Thermal density functional theory: Time-dependent linear response and approximate functionals from the fluctuation-dissipation theorem, *Phys. Rev. Lett.* **116**, 233001 (2016).

[56] R. Van Leeuwen, Mapping from densities to potentials in time-dependent density-functional theory, *Phys. Rev. Lett.* **82**, 3863 (1999).

[57] A. H. Skelt, K. Zawadzki, and I. D’Amico, Many-body effects on the thermodynamics of closed quantum systems, *J. Phys. A: Math. Theor.* **52**, 485304 (2019).

[58] K. Zawadzki, A. H. Skelt, and I. D’Amico, Approximating quantum thermodynamic properties using DFT, *J. Phys.: Condens. Matter* **34**, 274002 (2022).

[59] M. Herrera, K. Zawadzki, and I. D’Amico, Melting a Hubbard dimer: Benchmarks of ‘ALDA’ for quantum thermodynamics, *Eur. Phys. J. B* **91**, 248 (2018).

[60] M. Herrera, R. M. Serra, and I. D’Amico, DFT-inspired methods for quantum thermodynamics, *Sci. Rep.* **7**, 4655 (2017).

[61] A. Palamara, F. Plastina, A. Sindona, and I. D’Amico, Thermal-density-functional-theory approach to quantum thermodynamics, *Phys. Rev. A* **110**, 062203 (2024).

[62] H. J. D. Miller, M. H. Mohammady, M. Perarnau-Llobet, and G. Guarneri, Quantum thermodynamics of strongly coupled systems, *Phys. Rev. Lett.* **126**, 210603 (2021).

[63] V. Cavina, A. Mari, and V. Giovannetti, Quantum fluctuation theorems and work statistics in isolated systems, *Phys. Rev. Lett.* **119**, 050601 (2017).

[64] P. Abiuso and M. Perarnau-Llobet, Optimal work extraction and quantum thermodynamic bounds, *Phys. Rev. Lett.* **124**, 110606 (2020).

[65] B. Bhandari, P. T. Alonso, F. Taddei, F. von Oppen, R. Fazio, and L. Arrachea, Quantum thermodynamics of driven systems: Work, heat, and correlations, *Phys. Rev. B* **102**, 155407 (2020).

[66] K. Brandner and K. Saito, Thermodynamic bounds on precision in quantum nonequilibrium systems, *Phys. Rev. Lett.* **124**, 040602 (2020).

[67] J. Eglinton and K. Brandner, Thermodynamic uncertainty relations for quantum systems, *Phys. Rev. E* **105**, L052102 (2022).

[68] P. T. Alonso, P. Abiuso, M. Perarnau-Llobet, and L. Arrachea, Quantum thermodynamics in driven systems, *PRX Quantum* **3**, 010326 (2022).

[69] M. Scandi and M. Perarnau-Llobet, Thermodynamic bounds in quantum systems, *Quantum* **3**, 197 (2019).

[70] H. J. D. Miller, M. Scandi, J. Anders, and M. Perarnau-Llobet, Work statistics and fluctuation relations in many-body quantum systems, *Phys. Rev. Lett.* **123**, 230603 (2019).

[71] M. Campisi, S. Denisov, and P. Hänggi, Fluctuation relations for periodically driven quantum systems, *Phys. Rev. A* **86**, 032114 (2012).

[72] M. Scandi, H. J. D. Miller, J. Anders, and M. Perarnau-Llobet, Thermodynamics of quantum systems with strong correlations, *Phys. Rev. Res.* **2**, 023377 (2020).

[73] O. Onishchenko, G. Guarneri, P. Rosillo-Rodes, *et al.*, Probing coherent quantum thermodynamics using a trapped ion, arXiv:2207.14325 (2022).

[74] K. Zawadzki, A. Kiely, G. T. Landi, and S. Campbell, Non-gaussian work statistics at finite-time driving, *Phys. Rev. A* **107**, 012209 (2023).

[75] K. Zawadzki, R. M. Serra, and I. D’Amico, Work-distribution quantumness and irreversibility when crossing a quantum phase transition in finite time, *Phys. Rev. Res.* **2**, 033167 (2020).

[76] G. Guarneri, J. Eisert, and H. J. D. Miller, Generalized linear response theory for the full quantum work statistics, *Phys. Rev. Lett.* **133**, 070405 (2024).

[77] R. Kubo, Statistical-mechanical theory of irreversible processes. I. general theory and simple applications to magnetic and conduction problems, *J. Phys. Soc. Jpn.* **12**, 570 (1957).

[78] M. V. S. Bonança and S. Deffner, Quantum work and fluctuation theorems in driven systems, *J. Chem. Phys.* **140**, 244119 (2018).

[79] K. Burke and L. O. Wagner, Dft in a nutshell, *International Journal of Quantum Chemistry* **113**, 96 (2013).

[80] K. Burke, J. Werschnik, and E. Gross, Time-dependent density functional theory: Past, present, and future, *The Journal of chemical physics* **123** (2005).

[81] P. Talkner, E. Lutz, and P. Hänggi, Fluctuation theorems: Work is not an observable, *Phys. Rev. E* **75**, 050102 (2007).

[82] K. M. R. Audenaert, Comparisons between quantum state distinguishability measures, *Quantum Inf. Comput.* **14**, 31 (2014).

[83] S. Deffner and E. Lutz, Nonequilibrium entropy production for open quantum systems, *Phys. Rev. Lett.* **107**, 140404 (2011).

[84] P. Nazé and M. V. S. Bonança, Linear response for quantum work statistics in driven systems, *J. Stat. Mech.* , 013206 (2020).

[85] R. Kosloff and T. Feldmann, Discrete four-stroke quantum heat engine exploring the origin of friction, *Phys. Rev. E* **65**, 055102(R) (2002).

[86] F. Plastina, A. Alecce, T. J. G. Apollaro, *et al.*, Irreversible work and inner friction in quantum thermodynamic processes, *Phys. Rev. Lett.* **113**, 260601 (2014).

[87] A. Messiah, *Quantum Mechanics* (North-Holland, Amsterdam, 1970).

[88] H. Lehmann, On the properties of propagation functions and renormalization constants of quantized fields, *Il Nuovo Cimento (1955-1965)* **11**, 342 (1954).

[89] E. K. U. Gross and W. Kohn, Local density-functional theory of frequency-dependent linear response, *Phys. Rev. Lett.* **55**, 2850 (1985).

[90] T. V. Acconcia, M. V. S. Bonança, and S. Deffner, Quantum work statistics for driven systems, *Phys. Rev. E* **92**, 042148 (2015).

[91] F. Essler, H. Frahm, F. Göhmann, A. Klümper, and V. Korepin, *The One-Dimensional Hubbard Model* (Cambridge University Press, Cambridge, 2005).

[92] D. Pertot, A. Sheikhan, E. Cocchi, *et al.*, Relaxation dynamics of a Fermi gas in an optical superlattice, *Phys. Rev. Lett.* **113**, 170403 (2014).

[93] S. R. Manmana, V. Meden, R. M. Noack, and K. Schönhammer, Quantum correlations in one-dimensional systems: Density-matrix renormalization-group study, *Phys. Rev. B* **70**, 155111 (2004).

[94] L. Tincani, R. M. Noack, and D. Baeriswyl, Critical properties of the band-insulator-to-Mott-insulator transition in the strong-coupling limit of the ionic Hubbard model, *Phys. Rev. B* **79**, 165109 (2009).

[95] P. Roura-Bas, A. Camjayi, and M. J. Rozenberg, Mott, band, and charge-transfer insulators: A unified dynamical mean-field theory perspective, *Phys. Rev. B* **107**, 085108 (2023).

[96] D. J. Evans and D. J. Searles, The fluctuation theorem, *Adv. Phys.* **51**, 1529 (2002).

Appendix A: Benchmark of the LR-thTDDFT approach on the Hubbard dimer

To benchmark the performance of the LR-thTDDFT approach, we consider the exactly solvable two-site Hubbard model. As in the main text, we focus on the half-filled case with total spin projection along the z axis equal to zero, driven by a time-dependent external potential. The unperturbed Hamiltonian is given by

$$\hat{H}(t) = -J \sum_{i=1}^2 \sum_{\sigma=\uparrow,\downarrow} \left(\hat{c}_{i,\sigma}^\dagger \hat{c}_{i+1,\sigma} + \text{h.c.} \right) \quad (\text{A1})$$

$$+ U \sum_{i=1}^2 \hat{n}_{i,\uparrow} \hat{n}_{i,\downarrow} + v_0 (\hat{n}_1 - \hat{n}_2),$$

which is perturbed by a time-dependent external potential of the form

$$\hat{V}_{\text{ext}}(t) = \frac{\delta v_0 t}{\tau} (\hat{n}_1 - \hat{n}_2), \quad \delta v_0 \ll v_0. \quad (\text{A2})$$

We employed exactly the same computational strategy as in the main text, adopting the same approximation for the H_{xc} potential in the self-consistent solution of the KS equations, as well as for the kernel entering the response formalism. Benchmarks were performed in both the canonical and grand-canonical ensembles. As expected, owing to the finite size of the system (only two sites), small but appreciable differences arise between the two statistical ensembles.

In both ensembles, the overall agreement between the exact and thermal LR-TDDFT results is qualitatively and quantitatively very good, as shown in Figs. 3 and 4. This confirms the reliability of the approach in describing nonequilibrium

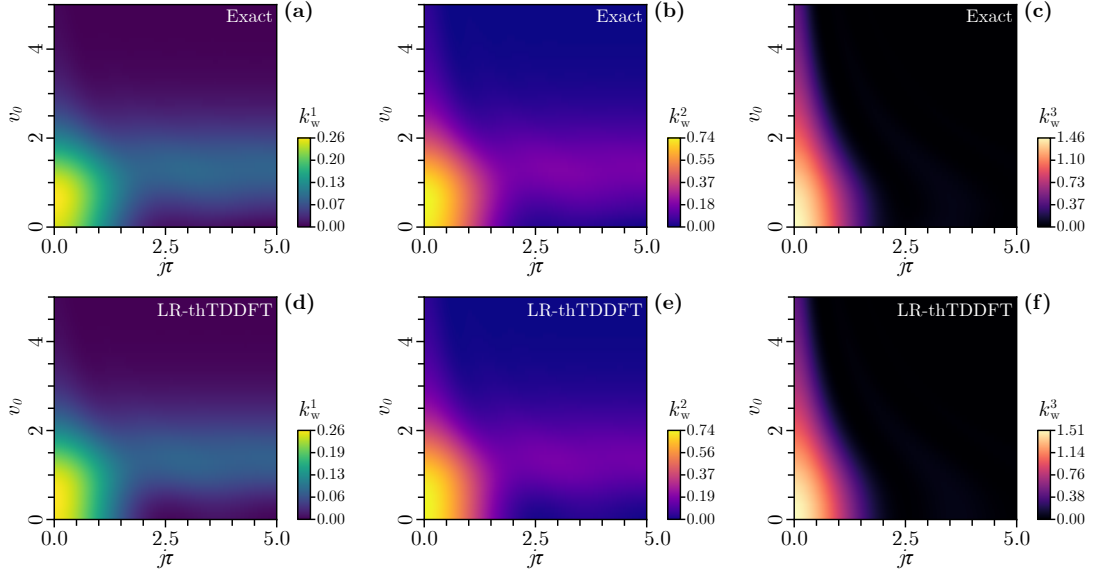


FIG. 3. Benchmark of the thermal LR-TDDFT approach against exact diagonalization for the two-site Hubbard model in the canonical ensemble at half filling and zero total spin projection. Panels (a)-(c) show the first three cumulants of the dissipated-work distribution obtained from exact diagonalization, while panels (e)-(g) show the corresponding results from LR-thTDDFT. The mean relative errors are approximately 1.36×10^{-2} for the first cumulant, 2.76×10^{-2} for the second, and 1.76×10^{-2} for the third.

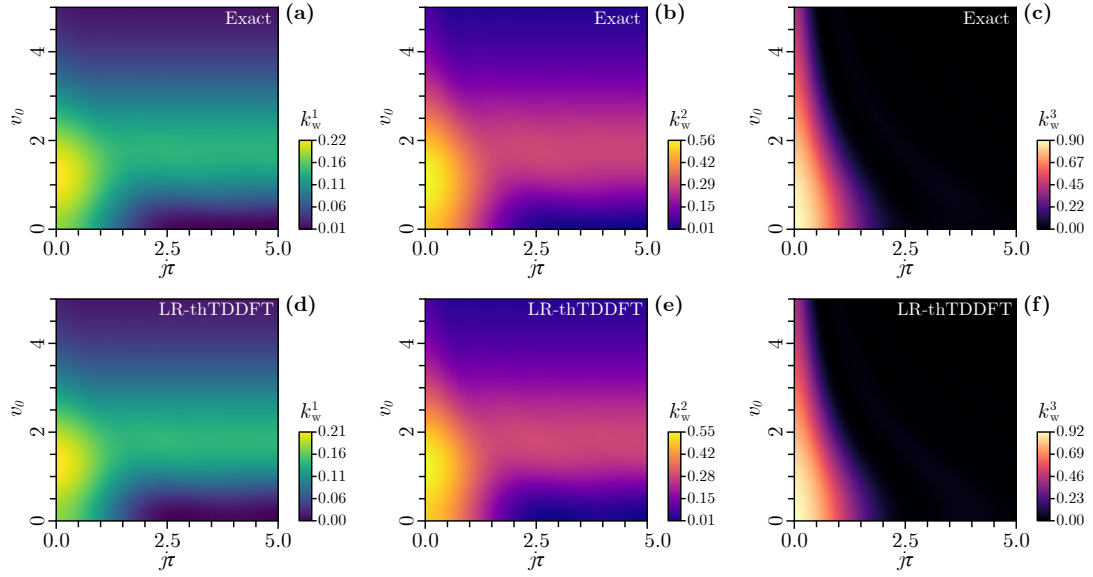


FIG. 4. Benchmark of the LR-thTDDFT approach against exact diagonalization for the two-site Hubbard model in the grand-canonical ensemble. The average relative errors between the exact and LR-thTDDFT results are approximately 1.20×10^{-2} for the first cumulant, 2.45×10^{-2} for the second, and 1.61×10^{-2} for the third. Despite the larger fluctuations expected in the grand-canonical setup, the agreement remains good, confirming the robustness of the thermal linear-response TDDFT approach.

thermodynamics even in strongly correlated regimes. Nevertheless, to further improve the level of approximation, one should go beyond the adiabatic local-density assumption and incorporate an explicit frequency dependence into the Hxc

kernel. Such an extension would enable the framework to capture the full spectrum of many-body excitations and dynamical correlations beyond the local and static limits.